

Article

Stereoselective Fluorescence Quenching in the Electron Transfer Photooxidation of Nucleobase-Related Azetidines by Cyanoaromatics

Ana B. Fraga-Timiraos, Gemma M. Rodríguez-Muñiz, Vicente Peiro-Penalba, Miguel A. Miranda * and Virginie Lhiaubet-Vallet *

Instituto Mixto de Tecnología Química (UPV-CSIC), Universitat Politècnica de València—Consejo Superior de Investigaciones Científicas, Avda de los Naranjos s/n, 46022 Valencia, Spain; anfrati@itq.upv.es (A.B.F.-T.); gemrodmu@itq.upv.es (G.M.R.-M.); vipeipe@etsii.upv.es (V.P.-P.)

* Correspondence: mmiranda@qim.upv.es (M.A.M.); lvirgini@itq.upv.es (V.L.-V.);

Tel.: +34-9-6387-7807 (M.A.M.); +34-9-6387-7815 (V.L.-V.); Fax: +34-9-6387-9447 (M.A.M. & V.L.-V.)

Academic Editor: Carlos E. Crespo-Hernández

Received: 15 October 2016; Accepted: 1 December 2016; Published: 7 December 2016

Abstract: Electron transfer involving nucleic acids and their derivatives is an important field in bioorganic chemistry, specifically in connection with its role in the photo-driven DNA damage and repair. Four-membered ring heterocyclic oxetanes and azetidines have been claimed to be the intermediates involved in the repair of DNA (6-4) photoproduct by photolyase. In this context, we examine here the redox properties of the two azetidine isomers obtained from photocycloaddition between 6-aza-1,3-dimethyluracil and cyclohexene. Steady-state and time-resolved fluorescence experiments using a series of photoreductants and photooxidants have been run to evaluate the efficiency of the electron transfer process. Analysis of the obtained quenching kinetics shows that the azetidine compounds can act as electron donors. Additionally, it appears that the *cis* isomer is more easily oxidized than its *trans* counterpart. This result is in agreement with electrochemical studies performed on both azetidine derivatives.

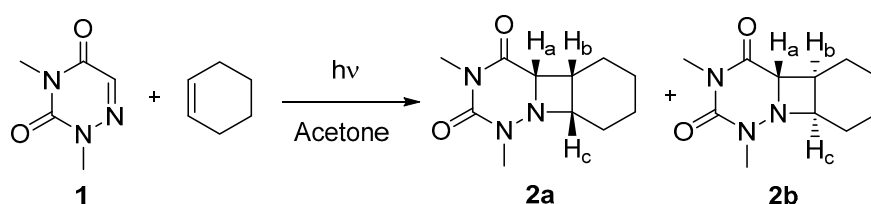
Keywords: DNA repair; energy and charge transfer; nucleobase analogues; photolyase; redox potential

1. Introduction

Electron transfer involving nucleic acids and their derivatives has been the subject of extensive studies in bioorganic chemistry, primarily because of its role in DNA damage and repair, but also in connection with the possible behavior of DNA as a molecular wire [1–9]. Last year, the Nobel Prize in Chemistry awarded for “the mechanistic studies of DNA repair” has emphasized, among others, the importance of photolyase enzymes [10]. They specifically repair bipyrimidine lesions, i.e., cyclobutane pyrimidine dimers (CPD) and (6-4) photoproducts, through a photochemically induced electron transfer from the catalytic flavin-adenosine cofactor to the lesion or to an oxetane/azetidine intermediate [5,11]. Although photorepair in Nature involves a reductive mechanism, the oxidative pathway is also relevant, particularly for long range mediated charge transport [1,12,13]. In this context, the photo-driven cycloreversion of CPD has been addressed through the use of photosensitized reductive or oxidative processes [12,14,15]. Moreover, radical ionic heterocycloreversion of 4-membered rings has emerged as an active field in the last two decades [8,9,16–19]. Oxetanes have been thoroughly investigated through both oxidative and reductive splitting; by contrast, little is known about thietanes and azetidines [9,16]. The latter are particularly relevant to the understanding of (6-4) photoproduct repair by photolyases at thymine-cytosine sequences. In a recent article, we have designed a model system obtained through photocycloaddition between thymine and 6-azauracil, demonstrating that photosensitizers with potential in the singlet excited state ranging from -3.3 V

to -2.1 V (vs. SCE) are appropriate photoreductants [20]. Interestingly, oxidative electron transfer has only been investigated with triphenylazetidines, which are structurally unrelated to pyrimidine bases [21].

With this background, the two azetidine isomers **2a** and **2b** were synthesized and used as substrates for investigating the initial step in reductive and oxidative electron transfer (Scheme 1). This process was studied by steady-state fluorescence using a series of photosensitizers (PS, Figure 1). Both electron donor and acceptor sensitizers were selected covering a large range of singlet excited state redox properties. They are namely *N,N*-dimethylaniline (DMA) and carbazole (CAR) for the photoreductants and 1,4-dicyanonaphthalene (DCN), 9,10-dicyanoanthracene (DCA) and 1-cyanonaphthalene (CNN) for the photooxidants (Table 1) [20,22]. Interestingly, and in contrast with our previous results on the thymine/azauracil dimers, the photooxidative process was more efficient. Moreover, a stereoselectivity in the fluorescence quenching was observed between *cis* and *trans* isomers.



Scheme 1. Synthesis of *cis* isomer **2a** and *trans* isomer **2b** from 6-aza-1,3-dimethyluracil (**1**).

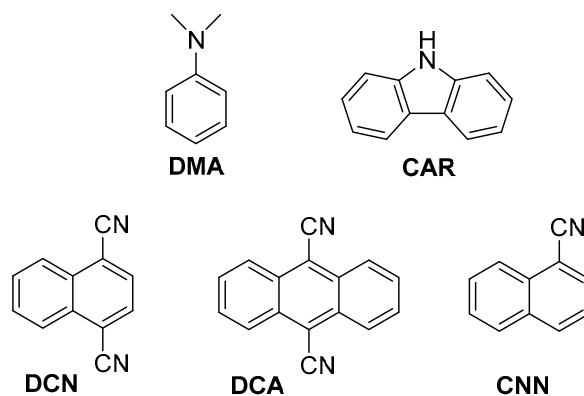


Figure 1. Structure of the used photosensitizers (PS).

2. Results

2.1. Synthesis

The synthesis of the azetidines **2a** and **2b** (Scheme 1) is described in details in the experimental section. Briefly, 6-aza-1,3-dimethyluracil (see NMR spectra in Figure S1), obtained from 6-azauracil through a known procedure [23], was irradiated (at $\lambda > 290$ nm) in the presence of cyclohexene using acetone as photosensitizer. The two isomers formed were separated by liquid chromatography. Their stereochemistry was determined from NMR analysis i.e., ^1H -, ^{13}C - spectra as well as HMQC and NOESY 2D experiments (see Figures S2–S5). A tentative assignment was proposed from the ^1H -NMR spectra because, in the case of the *cis* isomer, the H_a, H_b and H_c protons are located on the same side of the azetidine ring. Thus, H_a should be observed as a doublet as it is coupled to H_b. By contrast, in the *trans* isomer, H_a does not interact with the other two protons of the ring, and thus appears as a singlet at ca. 4.0 ppm. However, this signal cannot be observed clearly as it overlaps with H_c. The NOESY 2D NMR spectrum of **2a** is in agreement with the proposed *cis* configuration as an interaction was observed between the H_a and H_b protons located at 4.33 and 4.01 ppm, respectively (see Figure S4).

Preliminary experiments were performed to evaluate the UVA photoreactivity of **2a** and **2b** under reductive or oxidative conditions. Both isomers were consumed faster in the presence of photooxidant; moreover, it is noteworthy that the *cis* isomer **2a** was photodecomposed more efficiently than its *trans* counterpart **2b**.

2.2. Fluorescence Experiments

Steady-state fluorescence experiments were performed for the selected photosensitizers in order to evaluate the possibility of an electron transfer process with both azetidines. As stated above, electron donor and acceptor sensitizers were selected covering a large range of singlet excited state redox properties (see Table 1). They include DMA and CAR for the photoreductants and DCN, DCA and CNN for the photooxidants (Figure 1) [20,22]. Thus, acetonitrile solutions of the photosensitizer were prepared with an absorbance of ca. 0.15 at the excitation wavelength, which was fixed at $\lambda_{\text{exc}} = 310$ nm for DMA, CAR, DCN and CNN and $\lambda_{\text{exc}} = 375$ nm for DCA (see absorption spectra in Figure S6), and the fluorescence intensity was measured in the absence and in the presence of **2a** or **2b**. As observed in Figure 2, the emission spectra of CAR and DMA suffer only weak changes when azetidine is added, which signifies that electron injection is not an efficient process. By contrast, the photooxidant emissions underwent important quenching (Figure 2). In order to evaluate the efficiency of this oxidative electron transfer, time-resolved fluorescence was performed. Figure 3 shows the decays obtained for all the photosensitizers alone or in the presence of increasing amounts of compounds **2a** or **2b**. The singlet lifetime of all these photooxidants was shortened in the presence of azetidine derivatives. For example, the DCA lifetime reached values of 6.3 ns in the presence of 12.5 mM of **2a** (Figure 3c). Interestingly, this value was somewhat higher for **2b** (Figure 3d), being of ca. 7.2 ns. The bimolecular quenching rate constants (k_q , Table 1) were determined through Stern-Volmer analysis (see Materials and Methods) by plotting the ratio τ_0/τ , between the lifetime in the absence and in the presence of quencher, as a function of the quencher concentration [24]. The quenching process was more efficient as the reduction potential in the excited state (E^*) increased, which supports an electron transfer mechanism from the azetidine to the excited PS. Indeed, energy transfer can be ruled out because the absorption bands of **2a** and **2b** are below 300 nm (see Figure S7). Thus, their singlet energies (E_S) can be safely estimated to be >400 $\text{kJ}\cdot\text{mol}^{-1}$, that is more than 25 $\text{kJ}\cdot\text{mol}^{-1}$ higher than that of the highest E_S of the selected photosensitizer (Table 1).

Moreover, a significant difference of electron transfer efficiency was observed between **2a** and **2b** (see k_q , Table 1), the *cis* isomer being a more efficient quencher than the *trans* **2b**. The two isomers have the same bonds and connectivity; however, they differ in the arrangement of the dihydroazauracil and cyclohexane rings. A similar stereodifferentiation has previously been reported for photoreduction of the dimethylthymine cyclobutane dimer *cis-syn* and *trans-syn* diastereoisomers [25]. The more difficult reduction of the *cis-syn* isomer was attributed to a stereoelectronic effect as the formed anion radical suffers an unfavorable charge-dipole interaction with the carbonyl in C_4 of the other pyrimidine ring. Nevertheless, this explanation cannot be extended to **2a** and **2b** as the cyclohexane ring does not provide pronounced electronic effects, and the most likely explanation relies on different degrees of steric hindrance of the azetidine ring.

Table 1. Photophysical properties of the selected photosensitizers and their quenching rate constants by **2a** and **2b**.

PS	/ns	E^*/V	E_S ($\text{kJ}\cdot\text{mol}^{-1}$)	k_q (2a)/ 10^9 $\text{M}^{-1}\cdot\text{s}^{-1}$	k_q (2b)/ 10^9 $\text{M}^{-1}\cdot\text{s}^{-1}$
DMA	1.5	-3.0 ($\text{PS}^+\bullet/\text{PS}^*$) ¹	363	N.D. ³	N.D. ³
CAR	7.4	-2.5 ($\text{PS}^+\bullet/\text{PS}^*$) ¹	338	N.D. ³	N.D. ³
DCN	7.5	2.4 ($\text{PS}^*/\text{PS}\bullet^-$) ²	362	10	7.7
DCA	12.5	1.8 ($\text{PS}^*/\text{PS}\bullet^-$) ²	276	6.4	4.6
CNN	5.5	1.4 ($\text{PS}^*/\text{PS}\bullet^-$) ²	374	3.2	2.6

¹ From reference [20], vs. Ag/AgCl (saturated KCl). ² From reference [22], vs. Ag/AgNO₃. ³ N.D.: Not determined.

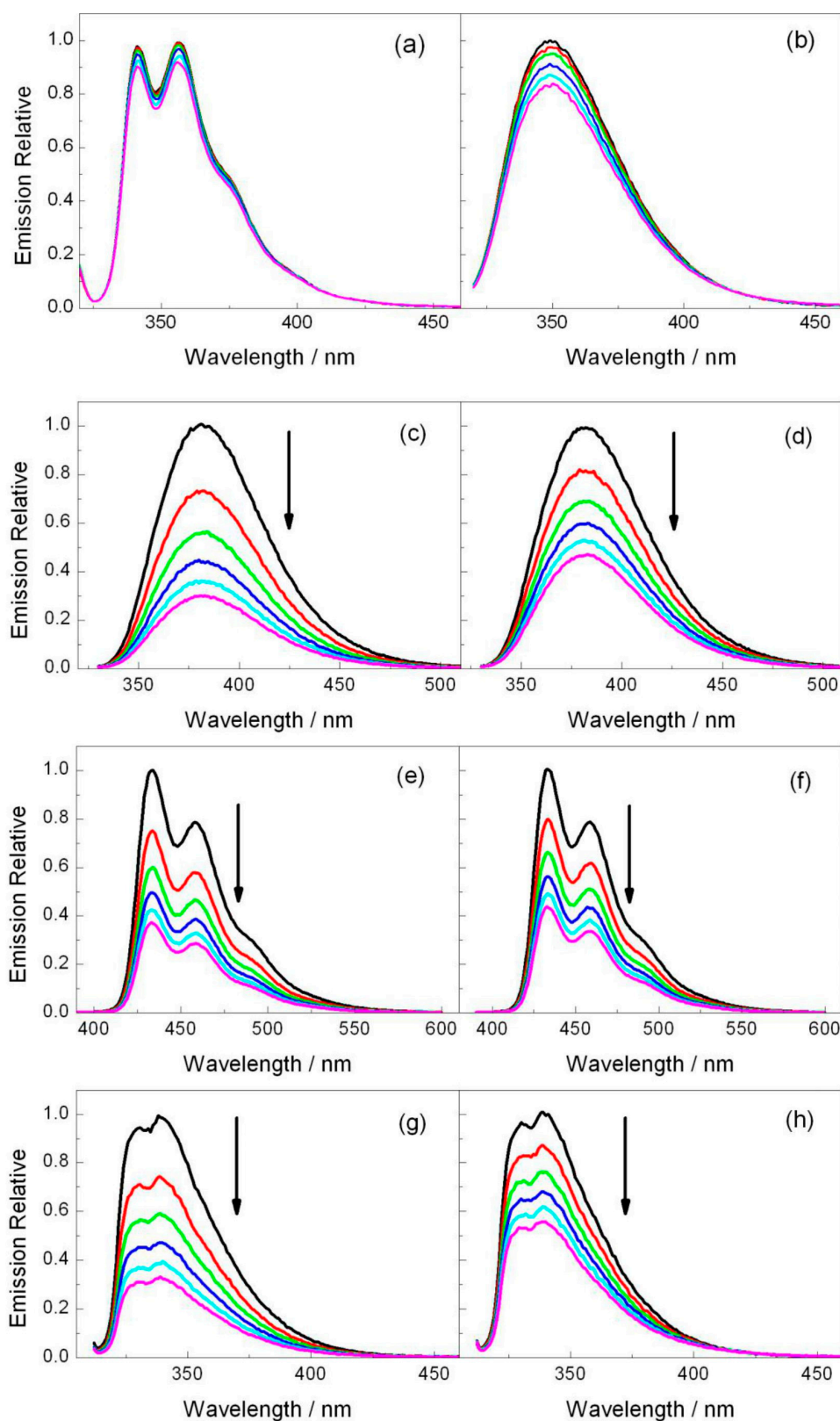


Figure 2. Fluorescence emission spectra for (a) CAR ($\lambda_{exc} = 310$ nm) and (b) DMA ($\lambda_{exc} = 310$ nm) in the presence of increasing amounts of **2b** (0–12.5 mM) as well as (c,d) DCN ($\lambda_{exc} = 310$ nm), (e,f) DCA ($\lambda_{exc} = 375$ nm), and (g,h) CNN ($\lambda_{exc} = 310$ nm) in the presence of increasing amounts of **2a** (left panel) or **2b** (right panel) (0–12.5 mM). The quencher concentration is 0 (black), 2.5 (red), 5 (green), 7.5 (blue), 10 (light blue) and 12.5 mM (pink).

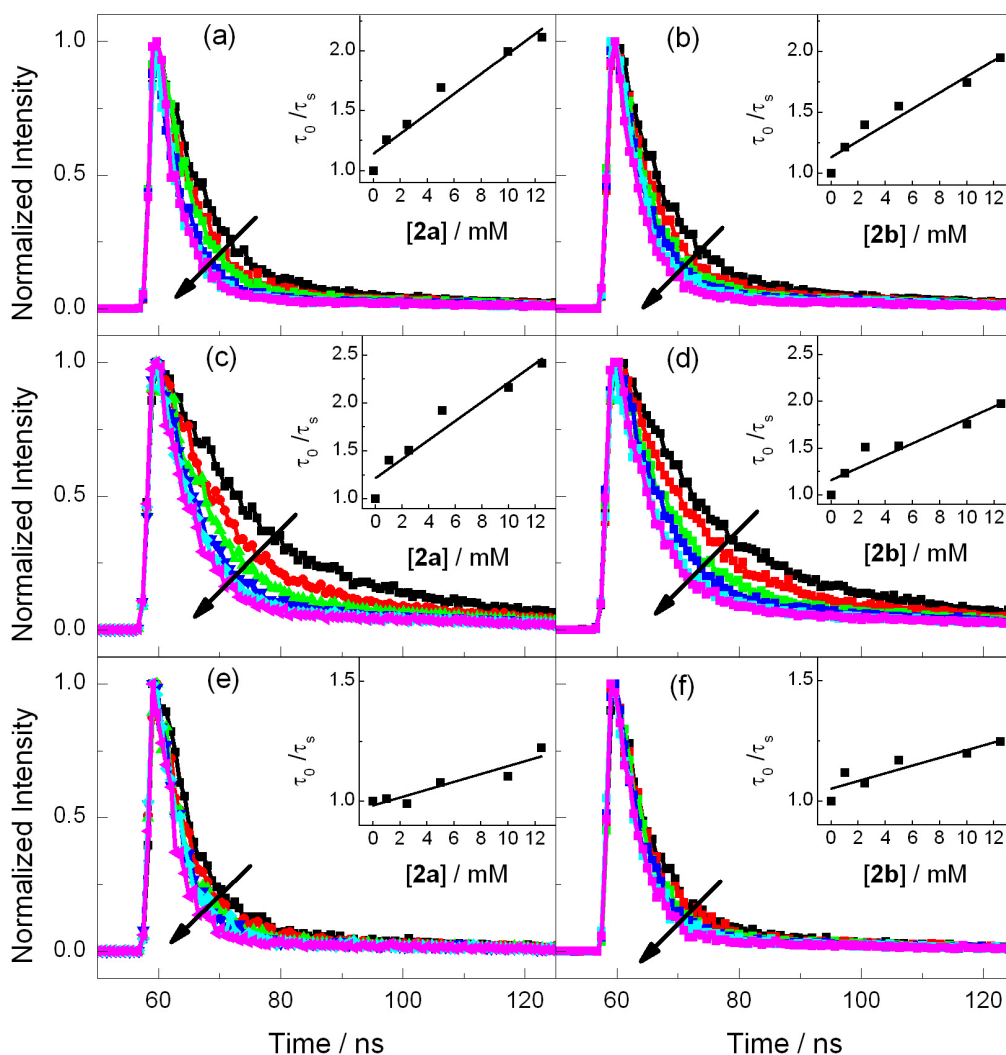


Figure 3. Fluorescence kinetic traces obtained for DCN ($\lambda_{\text{exc}} = 310$ nm) (a,b), DCA ($\lambda_{\text{exc}} = 375$ nm) (c,d) and CNN ($\lambda_{\text{exc}} = 310$ nm) (e,f) in the presence of increasing amounts of **2a** (left panel) or **2b** (right panel) from 0 to 12.5 mM. Inset: corresponding Stern Volmer plots. The quencher concentration is 0 (black), 2.5 (red), 5 (green), 7.5 (blue), 10 (light blue) and 12.5 mM (pink).

2.3. Electrochemistry

The different behavior observed between **2a** and **2b** must be connected with the redox properties of the two isomers. Thus, their electrochemical behavior was investigated by cyclic voltammetry using a three electrode standard configuration with two platinum wires as working and counter electrodes, and Ag/AgCl in saturated KCl as reference electrode. The cyclic voltammograms obtained at a scan rate of $0.5 \text{ V}\cdot\text{s}^{-1}$ are shown in Figure 4. A single wave was observed for both isomers, the oxidation being more difficult for **2b** than for **2a** as reflected by the more positive values of the peak potential ($E_p(\mathbf{2a}) = 1.30 \text{ V}$ and $E_p(\mathbf{2b}) = 1.55 \text{ V}$). This behavior is similar to that described for oxetanes or thietanes, where removal of one electron leads to cleavage of the heterocyclic 4-membered ring [9,17]. Moreover, the easier oxidation of **2a** is in full agreement with the photochemical results described in the previous section that established a more efficient electron transfer for the *cis* isomer.

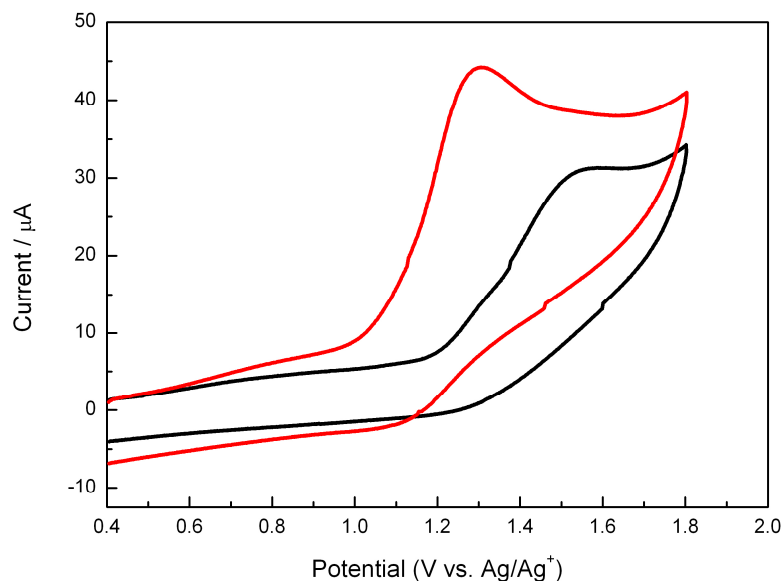


Figure 4. Cyclic voltammograms of **2a** (red line, 1 mM) and **2b** (black line, 1 mM) in acetonitrile using 0.1 M Bu_4NClO_4 as electrolyte. Scan rate: $0.5 \text{ V}\cdot\text{s}^{-1}$.

3. Materials and Methods

3.1. Chemicals

6-Azauracil, cyclohexene, CAR, DMA, DCN, DCA and CNN were purchased from Sigma-Aldrich (Madrid, Spain) and were used without further purification. Column chromatography was run with silica gel 60 A CC 35–70 μm as stationary phase, purchased from Merck (Madrid, Spain) and using analytical grade solvents obtained from Scharlau (Sentmenat, Spain). Acetonitrile HPLC grade (Scharlau) was used for fluorescence and electrochemical studies.

3.2. Instrumentation

NMR spectra were recorded on an AV 300 spectrometer (Bruker, Rivas-Vaciamadrid, Spain) at 296 K using CDCl_3 as solvent. Chemical shifts are referenced to the solvent signal i.e., 7.26 ppm and 77.2 ppm for ^1H -NMR and ^{13}C -NMR, respectively.

HRMS were obtained by electrospray mass spectroscopy in the positive mode mode using a Xevo QToF MS apparatus (Waters Corp., Cerdanyola del Vallès, Spain). The ESI source was operated in positive ionization mode with the capillary voltage at 1.9 kV. The temperature of the source and desolvation was set at 80 $^\circ\text{C}$ and 400 $^\circ\text{C}$, respectively. The cone and desolvation gas flows were 20 $\text{L}\cdot\text{h}^{-1}$ and 800 $\text{L}\cdot\text{h}^{-1}$, respectively. All data collected in Centroid mode were acquired using MasslynxTM software (V4.1 Waters Corp.). Leucine-enkephalin was used as the lock mass generating an $[\text{M} + \text{H}]^+$ ion (m/z 556.2771) at a concentration of 250 $\mu\text{g}/\text{mL}$ and flow rate of 50 $\mu\text{L}/\text{min}$ to ensure accuracy during the MS analysis.

Steady-state fluorescence experiments were carried out on a PTI LPS-220B spectrofluorometer (Photon Technology International, Longjumeau, France). Time-resolved fluorescence measurements were performed with a EasyLife V spectrometer from OBB (Palaiseau, France), equipped with a pulsed LED (λ_{exc} 310 nm or 375 nm) as excitation source; residual excitation signal was filtered in emission by using a cut-off filter (50% transmission at 320 nm or 400 nm for the 310 or 375 nm excitation, respectively). The kinetic traces were fitted by one monoexponential decay function, using a deconvolution procedure to separate them from the lamp pulse profile. All experiments were performed in a quartz cuvette of 1 cm of optical path.

Cyclic voltammetry measurements were performed with a VersaSTAT 3 potentiostat (Princeton Applied Research, Algete-Madrid, Spain) and using a three electrode standard configuration with two platinum wires as working and counter electrodes, and Ag/AgCl in saturated KCl as reference electrode. Measurements were carried out on an acetonitrile solution of **2a** or **2b** (1 mM) with 0.1 M Bu₄NClO₄ as electrolyte at a scan rate of 0.5 V·s⁻¹. All the solutions were previously purged with N₂ for at least 15 min before the measurements. Ferrocene were taken as internal standard and measured potentials have been referenced to the E_{1/2} potential of the ferrocinium/ferrocene (Fc⁺/Fc) couple of 0.425 V in CH₃CN [26].

3.3. Synthesis

1,3-Dimethyl-6-azauracil (1): 6-Azauracil (1.0 g, 8.84 mmol) was added to a suspension of NaH (0.5 g, 19.45 mmol) in anhydrous dimethylformamide (22 mL) at 0 °C. After stirring for 1 h at room temperature, the reaction mixture was treated with iodomethane (1.2 mL, 19.45 mmol) and stirred for 16 h. The solvent was removed, and the residue was purified by flash chromatography (silica gel, 100% dichloromethane) to give **1** (0.8 g, 70%) as a white solid powder. ¹H-NMR (300 MHz, CDCl₃) δ 7.36 (s, 1H), 3.63 (s, 3H), 3.33 ppm (s, 3H). ¹³C-NMR (75 MHz, CDCl₃) δ 156.4 (CO), 149.1 (CO), 133.9 (CH), 39.8 (CH₃), 27.0 ppm (CH₃).

1,3-Dimethyl-6-azauracilcyclohexene (2a, 2b). A solution of **1** (0.5 g, 3.54 mmol), acetone (10 mL) and cyclohexene (2.5 mL) in acetonitrile (30 mL) was placed in a Pyrex vessel (λ > 290 nm), purged with nitrogen and irradiated for 6 h using a medium pressure mercury lamp (750 W). The solvent was removed, and the residue was purified by flash chromatography (silica gel, 7% ethyl acetate/dichloromethane) to give two products as white solids.

2a (0.32 g, 41%): ¹H-NMR (300 MHz, CDCl₃) δ 4.33 (d, *J* = 9.0 Hz, 1H), 4.01 (apparent q, *J* = 8.5 Hz, 1H), 3.15 (s, 3H), 2.98 (s, 3H), 2.93 (m, 1H), 2.04–1.93 (m, 1H), 1.84–1.69 (m, 1H), 1.65–1.30 (m, 4H), 0.99–0.87 ppm (m, 2H). ¹³C-NMR (75 MHz, CDCl₃) δ 170.0 (CO), 152.5 (CO), 66.0 (CH), 63.9 (CH), 36.2 (CH), 30.4 (CH₃), 26.8 (CH₃), 23.3 (CH₂), 22.0 (CH₂), 21.4 (CH₂), 19.9 ppm (CH₂). HRMS (ESI): *m/z* calcd for C₁₁H₁₈N₃O₂ [M + H]⁺ 224.1399, found 224.1407.

2b (0.28 g, 36%): ¹H-NMR (300 MHz, CDCl₃) δ 4.03–3.91 (m, 2H), 3.24 (s, 3H), 3.19 (s, 3H), 2.42 (q, *J* = 8.8 Hz, 1H), 2.20–1.58 (m, 5H), 1.49–1.31 (m, 1H), 1.16–0.96 ppm (m, 1H). ¹³C-NMR (75 MHz, CDCl₃) δ 171.4 (CO), 151.9 (CO), 67.1 (CH), 66.9 (CH), 38.4 (CH), 33.0 (CH₃), 28.1 (CH₂), 27.4 (CH₂), 27.1 (CH₃), 22.2 (CH₂), 20.2 (CH₂). HRMS (ESI): *m/z* calcd for C₁₁H₁₈N₃O₂ [M + H]⁺ 224.1399, found 224.1392.

3.4. Fluorescence Quenching

The absorbance of the sensitizer for the fluorescence experiments was kept 0.15 at the excitation wavelength (λ_{exc} = 310 nm for CAR, DMA, DCN and CNN, or 375 nm for DCA). On the other hand, a stock solution of azetidine **2a** or **2b** (0.15 M) was prepared, so it was only necessary to add microliter volumes to the sample cell to obtain appropriate concentration of the quencher. The rate constants (k_q) for the reaction were obtained from the Stern-Volmer plots [24] following Equation (1):

$$1/\tau = 1/\tau_0 + k_q \times [\mathbf{2a}] \quad \text{or} \quad 1/\tau = 1/\tau_0 + k_q \times [\mathbf{2b}] \quad (1)$$

where τ₀ is the lifetime of the photosensitizer in the absence of **2a** or **2b** and τ is the lifetime after addition of a quencher concentration [**2a**] or [**2b**].

4. Conclusions

The initial electron transfer step assumed to be involved in the repair of thymine-cytosine (6-4) photoproducts by photolyases has been investigated here by using azetidines **2a** or **2b** and photosensitizers DMA, CAR, DCN, DCA and CNN as model compounds. The fluorescence of DMA and CAR is hardly quenched by **2a** or **2b**, indicating that the photoreductive pathway is not efficient in

the corresponding donor-acceptor pairs. Conversely, an efficient fluorescence quenching is observed for the cyanoaromatics DCN, DCA and CNN, both in steady-state and time-resolved experiments. The dynamic quenching supports an efficient oxidative electron transfer, which is faster for the *cis* isomer **2a**. Electrochemical studies are in agreement with these results, showing that oxidation of **2a** is easier due to its more favorable redox potential.

Supplementary Materials: Supplementary materials can be accessed at: <http://www.mdpi.com/1420-3049/21/12/1683/s1>.

Acknowledgments: Spanish Government (CTQ2015-70164-P, RIRAAF RETICS RD12/0013/0009, Red de Fotoquímica Biológica CTQ2015-71896-REDT, Severo Ochoa program/SEV-2012-0267 and SVP-2013-068057 for A. B. F.-R. grant) and Generalitat Valenciana (Prometeo II/2013/005) are gratefully acknowledged.

Author Contributions: V.P.-P. made the preliminary experiments; A.B.F.-T. performed the experiments and analyzed the data; G.M.R.-M. supervised the laboratory work; V.L.-V. and M.A.M. conceived, designed the experiments and wrote the paper.

Conflicts of Interest: The authors declare no conflict of interest. The founding sponsors had no role in the design of the study; in the collection, analyses, or interpretation of data; in the writing of the manuscript, and in the decision to publish the results.

References

1. Arnold, A.R.; Grodick, M.A.; Barton, J.K. DNA charge transport: From chemical principles to the cell. *Cell Chem. Biol.* **2016**, *23*, 183–197. [[CrossRef](#)] [[PubMed](#)]
2. Jia, C.; Ma, B.; Xin, N.; Guo, X. Carbon electrode–molecule junctions: A reliable platform for molecular electronics. *Acc. Chem. Res.* **2015**, *48*, 2565–2575. [[CrossRef](#)] [[PubMed](#)]
3. Beratan, D.N.; Liu, C.; Migliore, A.; Polizzi, N.F.; Skourtis, S.S.; Zhang, P.; Zhang, Y. Charge transfer in dynamical biosystems, or the treachery of (static) images. *Acc. Chem. Res.* **2015**, *48*, 474–481. [[CrossRef](#)] [[PubMed](#)]
4. Kawai, K.; Majima, T. Hole transfer kinetics of DNA. *Acc. Chem. Res.* **2013**, *46*, 2616–2625. [[CrossRef](#)] [[PubMed](#)]
5. Sancar, A. Structure and function of DNA photolyase and cryptochrome blue-light photoreceptors. *Chem. Rev.* **2003**, *103*, 2203–2238. [[CrossRef](#)] [[PubMed](#)]
6. Kanvah, S.; Joseph, J.; Schuster, G.B.; Barnett, R.N.; Cleveland, C.L.; Landman, U. Oxidation of DNA: Damage to nucleobases. *Acc. Chem. Res.* **2010**, *43*, 280–287. [[CrossRef](#)] [[PubMed](#)]
7. Kelley, S.O.; Barton, J.K. Electron transfer between bases in double helical DNA. *Science* **1999**, *283*, 375–381. [[CrossRef](#)] [[PubMed](#)]
8. Breeger, S.; von Meltzer, M.; Hennecke, U.; Carell, T. Investigation of the pathways of excess electron transfer in DNA with flavin-donor and oxetane-acceptor modified DNA hairpins. *Chem. Eur. J.* **2006**, *12*, 6469–6477. [[CrossRef](#)] [[PubMed](#)]
9. Bouscicault, F.; Robert, M. Electron transfer in DNA and in DNA-related biological processes. Electrochemical insights. *Chem. Rev.* **2008**, *108*, 2622–2645. [[CrossRef](#)] [[PubMed](#)]
10. Gustafsson, C.M. The Nobel Prize in Chemistry 2015—Advanced Information. Available online: http://www.nobelprize.org/nobel_prizes/chemistry/laureates/2015/advanced.html (accessed on 2 December 2016).
11. Brettel, K.; Byrdin, M. Reaction mechanisms of DNA photolyase. *Curr. Opin. Struct. Biol.* **2010**, *20*, 693–701. [[CrossRef](#)] [[PubMed](#)]
12. Dandliker, P.J.; Holmlin, R.E.; Barton, J.K. Oxidative thymine dimer repair in the DNA helix. *Science* **1997**, *275*, 1465–1468. [[CrossRef](#)] [[PubMed](#)]
13. Vicic, D.A.; Odom, D.T.; Núñez, M.E.; Gianolio, D.A.; McLaughlin, L.W.; Barton, J.K. Oxidative repair of a thymine dimer in DNA from a distance by a covalently linked organic intercalator. *J. Am. Chem. Soc.* **2000**, *122*, 8603–8611. [[CrossRef](#)]
14. Hartman, T.; Cibulka, R. Photocatalytic systems with flavinium salts: From photolyase models to synthetic tool for cyclobutane ring opening. *Org. Lett.* **2016**, *18*, 3710–3713. [[CrossRef](#)] [[PubMed](#)]
15. Scannell, M.P.; Fenick, D.J.; Yeh, S.-R.; Falvey, D.E. Model studies of DNA photorepair: Reduction potentials of thymine and cytosine cyclobutane dimers measured by fluorescence quenching. *J. Am. Chem. Soc.* **1997**, *119*, 1971–1977. [[CrossRef](#)]

16. Pérez-Ruiz, R.; Jiménez, M.C.; Miranda, M.A. Hetero-cycloreversions mediated by photoinduced electron transfer. *Acc. Chem. Res.* **2014**, *47*, 1359–1368. [[CrossRef](#)] [[PubMed](#)]
17. Boussicault, F.; Robert, M. Electrochemical approach to the repair of oxetanes mimicking DNA (6-4) photoproducts. *J. Phys. Chem. B* **2006**, *110*, 21987–21993. [[CrossRef](#)] [[PubMed](#)]
18. Prakash, G.; Falvey, D.E. Model studies of the (6-4) photoproduct DNA photolyase: Synthesis and photosensitized splitting of a thymine-5,6-oxetane. *J. Am. Chem. Soc.* **1995**, *117*, 11375–11376. [[CrossRef](#)]
19. Friedel, M.G.; Cichon, M.K.; Carell, T. Model compounds for (6-4) photolyases: A comparative flavin induced cleavage study of oxetanes and thietanes. *Org. Biomol. Chem.* **2005**, *3*, 1937–1941. [[CrossRef](#)] [[PubMed](#)]
20. Fraga-Timiraos, A.B.; Lhiaubet-Vallet, V.; Miranda, M.A. Repair of a dimeric azetidines related to the thymine–cytosine (6-4) photoproduct by electron transfer photoreduction. *Angew. Chem. Int. Ed.* **2016**, *55*, 6037–6040. [[CrossRef](#)] [[PubMed](#)]
21. Andreu, I.; Delgado, J.; Espinós, A.; Pérez-Ruiz, R.; Jiménez, M.C.; Miranda, M.A. Cycloreversion of azetidines via oxidative electron transfer. Steady-state and time-resolved studies. *Org. Lett.* **2008**, *10*, 5207–5210. [[CrossRef](#)] [[PubMed](#)]
22. Pac, C.; Ohtsuki, T.; Shiota, Y.; Yanagida, S.; Sakurai, H. Photochemical reactions of aromatic compounds. XLII. Photosensitized reactions of some selected diarylcyclobutanes by aromatic nitriles and chloranil. Implications of charge-transfer contributions on exciplex reactivities. *Bull. Chem. Soc. Jpn.* **1986**, *59*, 1133–1139. [[CrossRef](#)]
23. Swenton, J.S.; Hyatt, J.A. Photosensitized cycloadditions to 1,3-dimethyl-6-azauracil and 1,3-dimethyl-6-azathymine. Imine linkage unusually reactive toward photocycloaddition. *J. Am. Chem. Soc.* **1974**, *96*, 4879–4885. [[CrossRef](#)] [[PubMed](#)]
24. Stern, O.; Volmer, M. Über die abklingungszeit der fluoreszenz. *Physik. Z.* **1919**, *20*, 183–188.
25. Scannell, M.P.; Prakash, G.; Falvey, D.E. Photoinduced electron transfer to pyrimidines and 5,6-dihydropyrimidine derivatives: Reduction potentials determined by fluorescence quenching kinetics. *J. Phys. Chem. A* **1997**, *101*, 4332–4337. [[CrossRef](#)]
26. Pavlishchuk, V.V.; Addison, A.W. Conversion constants for redox potentials measured versus different reference electrodes in acetonitrile solutions at 25 degrees C. *Inorg. Chim. Acta* **2000**, *298*, 97–102. [[CrossRef](#)]

Sample Availability: Samples of the compounds **2a** or **2b** are available from the authors.



© 2016 by the authors; licensee MDPI, Basel, Switzerland. This article is an open access article distributed under the terms and conditions of the Creative Commons Attribution (CC-BY) license (<http://creativecommons.org/licenses/by/4.0/>).